Available online at www.sciencedirect.com

ScienceDirect

J. Differential Equations 257 (2014) 1662–1688

Journal of Differential Equations

www.elsevier.com/locate/jde

Bifurcations and complex dynamics of an SIR model with the impact of the number of hospital beds ☆

Chunhua Shan, Huaiping Zhu *

Department of Mathematics and Statistics, York University, Toronto, ON, M3J 1P3, Canada

Received 14 July 2012; revised 9 April 2014

Available online 3 June 2014

Abstract

In this paper we establish an SIR model with a standard incidence rate and a nonlinear recovery rate, formulated to consider the impact of available resource of the public health system especially the number of hospital beds. For the three dimensional model with total population regulated by both demographics and diseases incidence, we prove that the model can undergo backward bifurcation, saddle-node bifurcation, Hopf bifurcation and cusp type of Bogdanov–Takens bifurcation of codimension 3. We present the bifurcation diagram near the cusp type of Bogdanov–Takens bifurcation point of codimension 3 and give epidemiological interpretation of the complex dynamical behaviors of endemic due to the variation of the number of hospital beds. This study suggests that maintaining enough number of hospital beds is crucial for the control of the infectious diseases.

Keywords: SIR model; Nonlinear recovery rate; Number of hospital beds; Dynamics; Backward bifurcation; Saddle-node bifurcation; Hopf bifurcations; Bogdanov–Takens bifurcations

1. Introduction

There is a long and distinguished history of mathematical modeling in epidemiology since Bernoulli developed the first dynamic model of smallpox spread in 1760 [3]. The study

☆ This research was supported by NSERC and ERA, an Early Researcher Award of Ministry of Research and Innovation of Ontario, Canada.

* Corresponding author.
E-mail address: huaiping@mathstat.yorku.ca (H. Zhu).

http://dx.doi.org/10.1016/j.jde.2014.05.030
0022-0396/

of epidemiological models reveals the underlying mechanisms that influence the transmission and control of infectious diseases. Among numerous epidemiological models, the SIR type of compartmental models and Ross–MacDonald models have played a critical role in the development of modern mathematical epidemiology, and mathematical modeling approach has become an important tool in understanding the dynamics and mechanisms of disease transmission for the purpose of control and prevention of infectious diseases [1,3,6].

In modeling of infectious diseases, there are several factors that substantially affect the dynamical behavior of the models such as the demographics of involving populations, incidence rate and recovery rate. In the classic SIR models, the simple mass action incidence rate or the standard incidence rate $\frac{\beta S(t)I(t)}{N(t)}$ and linear recovery rate $\mu I(t)$ are used, where $S(t)$, $I(t)$ and $R(t)$ are the numbers of susceptible, infectious and recovered individuals at time t, respectively. $N(t) = S(t) + I(t) + R(t)$ is the number of the total populations. The constant β is the average number of adequate contacts per unit time with infectious individuals, and the constant μ is the per capita recovery rate of infectious individuals. For classic epidemiological models with different demographics, typically they do not have bistability and periodicity, and the dynamics are almost completely characterized by the so called basic reproduction numbers $\mathbb{R}_0$. The disease will be eliminated if $\mathbb{R}_0 < 1$, otherwise the disease will persist [3,6,10,14].

In practice, multiple peaks or periodic oscillations are observed during the transmission of many infectious disease. Lots of studies have shown that the nonlinear incidence rate plays a crucial role in producing the rich dynamics of epidemic models including periodic oscillations [4,5,9,10,12–16] etc. The saturated incidence rate $g(I)S$ is introduced into the epidemic model by Capasso and Serio [4]. The nonlinear incidence rate $\kappa I^p S^q$ ($\kappa, p, q > 0$) is investigated by Liu et al. [12,13]. The effect of behavioral changes has been incorporated by Liu using the nonlinear incidence rate $\frac{\kappa I^l S}{1+\alpha I^h}$ with $\kappa, l, \alpha, h > 0$, and studied by Liu et al. [12,13] and Ruan and their colleagues [15,16]. Generalized form of nonlinear incidence rate is considered by Derrick and van den Driessche [5].

The SIR and SIRS models always assume that the total population size remains or asymptotically approaches a constant. This assumption is reasonable when the disease spreads quickly and dies out within a short time or the disease rarely causes deaths, which can help to reduce the model into a planar system to make the mathematical analysis easier as many tools can be used for the planar system. However, it is not reasonable when the natural birth and death rate are not balanced or when the disease-induced deaths are significant such as plague, measles, scarlet fever, diphtheria, tuberculosis, smallpox, malaria etc. In this study, we suppose the diseased-induced death rate $\nu > 0$ so that the human populations will be regulated by both the demographics and infectious diseases.

In this paper we consider the following SIR model with the standard incidence rate [14]

$$\begin{cases} \dfrac{dS}{dt} = A - dS - \dfrac{\beta SI}{S+I+R}, \\ \dfrac{dI}{dt} = -(d+\nu)I - \mu I + \dfrac{\beta SI}{S+I+R}, \\ \dfrac{dR}{dt} = \mu I - dR, \end{cases} \tag{1.1}$$

where $A > 0$ is the recruitment rate of susceptible population; $d > 0$ is the per capita natural death rate of the population; $\nu > 0$ is the per capita disease-induced death rate; $\mu > 0$ is the per capita recovery rate of infectious individuals.

The recovery rate μ, or the exit rate is usually taken as a constant in previous modeling, but in practice it depends on the time of recovering process, which can be related to the total infectious individuals seeking treatment, and we will formulate it to incorporate the impact of available resources of health system to the public, in particular the number of the hospital beds which will be elaborated in Section 2. Our analysis and results show that the nonlinear recovery rate of SIR model can lead to rich and complex dynamics such as backward bifurcation, saddle-node bifurcation, Hopf bifurcation, homoclinic bifurcation and cusp type of Bogdanov–Takens bifurcation of codimension 3. The rich and complex dynamics of the model indicate that maintaining a critical number of hospital beds is crucial to the control of infectious disease.

The Bogdanov–Takens bifurcation of codimension 2 was found and studied in the epidemic models with nonlinear incidence rate [15,16]. The cusp type of Bogdanov–Takens bifurcation of codimension 3 was firstly studied in the predator–prey system with generalized Holling types III and IV functional response [11,20]. Among the epidemiological models, this kind of bifurcation was only investigated in [16] for the SIRS model with a saturated incidence rate, and the study was carried out for a planar system by assuming that the total population remains a constant. As far as we know, the higher codimension bifurcations, including Bogdanov–Takens bifurcation of codimension greater than or equal to 2, are studied directly for the planar system using the qualitative and bifurcation theory. In this paper, we will study the cusp type of Bogdanov–Takens bifurcation of codimension 3 in three dimensional phase space as system (1.1) cannot be reduced to the planar system by decoupling one variable.

This paper is organized as follows. In Section 2, we formulate the nonlinear recovery rate μ to incorporate the impact of the number of hospital beds into the SIR model. In Section 3, we study the existence and types of the equilibria. In Section 4, we study the backward bifurcation, saddle-node bifurcation, Hopf bifurcation and the cusp type of Bogdanov–Takens bifurcation of codimension 2 and 3. We give the bifurcation diagram based on our analytic analysis and simulation near the cusp point of order 3. We summarize our results and indicate the epidemiological significance of the number of hospital beds in Section 5.

2. SIR model incorporating the number of hospital beds

In classical epidemic models, the per capita recovery rate μ is assumed to be a constant, but in general, the recovery rate μ depends on the resources of the health system available to the public, particularly the capacity of the hospital settings and effectiveness and efficiency of the treatment. There are many factors determining the recovery rate. The primary factor is the number of health workforce including physicians, nurses, pharmacists and other health care workers (HCW). The facilities of the hospital such as medical apparatus and equipment, the number of the hospital beds and medicines are another significant factors which are essential for safe and effective prevention, diagnosis and treatment of illness [19,21].

Among these factors, hospital bed-population ratio (HBPR), the number of available hospital beds per 10,000 population is used by health planners as a method of estimating resource availability to the public [2,19,21]. The rationale is given by WHO Statistical Information System (WHOSIS) [19,21], and we directly quote it in the following:

Service delivery is an important component of health systems. To capture availability, access and distribution of health services delivery a range of indicators or a composite indicator is needed. Currently, there is no such data for the majority of countries. In-patient beds density is one of the few available indicators on a component of level of health service delivery.

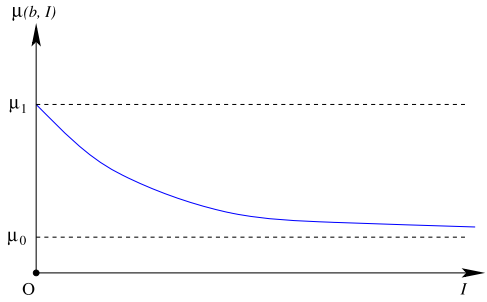

Fig. 1. The curve of recovery rate $\mu(b, I)$ with form (2.1) for a given number of hospital beds b.

The data about the hospital bed-population ratio (HBPR) in different countries or regions is released annually in World Health Statistics annual reports by WHO [19].

Due to the significance of HBPR, as a preliminary study of this topic we will formulate the recovery rate μ incorporating the impact of the capacity and limit resources of the health care system in terms of HBPR denoted as the parameter $b > 0$. On the other hand, μ depends on the number of the infectious individuals I, so μ is a function of b and I. In general, for the per capita recovery rate $\mu(b, I)$, we can assume

- $\mu(b, I) > 0$ for $I \geq 0$, $b > 0$, and $\mu(b, 0) = \mu_1 > 0$, where μ_1 is the maximum per capita recovery rate due to the sufficient health care resource and few infectious individuals as well as the inherent property of a specific disease.
- $\frac{\partial \mu(b,I)}{\partial I} < 0$, $\lim_{I\to\infty} \mu(b, I) = \mu_0 > 0$ and $\lim_{I\to 0} \mu(b, I) = \mu(b, 0) = \mu_1$. It is natural that $\mu(b, I)$ is a decreasing function of I. Furthermore if the number of new infectious individuals becomes larger and larger, the available resources of the hospital cannot satisfy such large demand for treatment, yet it is still possible that a certain amount of infectious individuals can be treated and get recovered, and the minimum recovery rate can be sustained. Therefore, we assume that $\lim_{I\to\infty} \mu(b, I) = \mu_0$. Here μ_0 is the minimum per capita recovery rate due to the function of basic clinical resources.
- $\frac{\partial \mu(b,I)}{\partial b} > 0$, $\lim_{b\to\infty} \mu(b, I) = \mu_1$ and $\lim_{b\to 0} \mu(b, I) = \mu_0$. The per capita recovery rate is the increasing function of b, which is bounded by μ_0 and μ_1 for any $b > 0$.

Generally, according to the above assumption, one can use different functions to model the impact of hospital resource on the recovery rate, and we study it with a simple function

$$\mu = \mu(b, I) = \mu_0 + (\mu_1 - \mu_0)\frac{b}{I + b}, \tag{2.1}$$

as shown in Fig. 1. The medium recovery rate can be achieved when $I = b$, so the parameter b as a measure of available hospital resources, namely, the number of hospital beds plays an important role in controlling the spread of infectious diseases. Therefore we study the following system

$$\begin{cases} \dfrac{dS}{dt} = A - dS - \dfrac{\beta SI}{S + I + R}, \\ \dfrac{dI}{dt} = -(d + \nu)I - \mu(b, I)I + \dfrac{\beta SI}{S + I + R}, \\ \dfrac{dR}{dt} = \mu(b, I)I - dR, \end{cases} \tag{2.2}$$

with $\mu(b, I)$ defined in (2.1) and initial value

$$S(0) = S_0, \qquad I(0) = I_0, \qquad R(0) = R_0.$$

For the system (2.2) the cone R^{3+} is positively invariant. The C^1 smoothness of the right side of system (2.2) implies the local existence and uniqueness of the solution with the initial values in R^{3+}.

Summing up the three equations of system (2.2), we obtain $N'(t) = A - dN - \nu I$, therefore all solutions in the first octant approach, enter or stay inside the set defined by

$$D = \left\{ (S, I, R) \,\middle|\, S \geq 0, I \geq 0, R \geq 0, S + I + R \leq \frac{A}{d} \right\},$$

so they are eventually bounded and hence globally exist. Thus the initial value problem of system (2.2) is mathematically well posed and epidemiologically reasonable since all variables remain nonnegative.

Because the total population $N(t)$ is regulated by the disease, we cannot reduce the system to a lower dimensional system, hence we analyze system (2.2) in three dimensional phase space.

3. Existence and types of equilibria

3.1. Existence of equilibria

We find equilibria by setting the right hand side of system (2.2) equal to zero. One trivial equilibrium point is the disease free equilibrium (DFE), which we denote by $E_0(\frac{A}{d}, 0, 0)$. For E_0, use the formula in [17] to calculate the basic reproduction number

$$\mathbb{R}_0 = \frac{\beta}{d + \nu + \mu_1}. \tag{3.1}$$

For any endemic equilibrium $E(S, I, R)$, its coordinates satisfy

$$S(I) = \frac{A - (d + \nu + \mu(b, I))I}{d}, \qquad R(I) = \frac{\mu(b, I)I}{d}, \tag{3.2}$$

and the coordinate I should be the positive root of the quadratic equation

$$f(I) = \mathscr{A} I^2 + \mathscr{B} I + \mathscr{C}, \tag{3.3}$$

where

$$\begin{aligned}
\mathscr{A} &= (d + \nu + \mu_0)(\beta - \nu), \\
\mathscr{B} &= (d + \nu + \mu_0 - \beta)A + (\beta - \nu)(d + \nu + \mu_1)b, \\
\mathscr{C} &= (d + \nu + \mu_1)Ab(1 - \mathbb{R}_0).
\end{aligned}$$

The equation $f(I) = 0$ may have two roots if $\Delta_0 > 0$ which are denoted as

$$I_1 = \frac{-\mathscr{B} - \sqrt{\Delta_0}}{2\mathscr{A}}, \qquad I_2 = \frac{-\mathscr{B} + \sqrt{\Delta_0}}{2\mathscr{A}},$$

where

$$\Delta_0 = (\beta - \nu)^2\delta_1^2 b^2 - 2A(\beta - \nu)\big[\beta(\mu_1 - \mu_0) + \delta_0(\delta_1 - \beta)\big]b + A^2(\beta - \delta_0)^2.$$

Here $\delta_0 = d + \nu + \mu_0$ and $\delta_1 = d + \nu + \mu_1$. We will only use these two notations δ_0 and δ_1 in Section 4.1 and Section 5.

If $\Delta_0 = 0$, there will be a unique root of $f(I) = 0$ with multiplicity 2 denoted as $I^* = \frac{-\mathscr{B}}{2\mathscr{A}}$. As we study the equilibrium in the positive cone R^{3+}, the constrain that $S(I) > 0$ and $R(I) > 0$ requires the coordinate I should satisfy the inequality

$$g(I) \triangleq -(d + \nu + \mu_0)I^2 + \big(A - (d + \nu + \mu_1)b\big)I + Ab > 0.$$

We study the existence of equilibria in the following three cases.

(i) $\mathbb{R}_0 > 1$.

In this case $\beta > d + \nu + \mu_1$, then $\mathscr{A} > 0$, $\mathscr{C} < 0$ and $\Delta_0 > 0$, so $I_1 < 0, I_2 > 0$. One can verify $g(I_2) > 0$, so system (2.2) has a unique endemic equilibrium $E_2 = (S(I_2), I_2, R(I_2))$.

(ii) $\mathbb{R}_0 = 1$.

In this case $\beta = d + \nu + \mu_1$, then $\mathscr{A} > 0$ and $\mathscr{C} = 0$, so Eq. (3.3) has two roots, 0 and $-\frac{\mathscr{B}}{\mathscr{A}}$. Therefore system (2.2) has a unique endemic equilibrium $E_2 = (S(I_2), I_2, R(I_2))$ if and only if $\mathscr{B} < 0$.

(iii) $\mathbb{R}_0 < 1$.

If $\beta < \nu$, then $\mathscr{A} < 0, \mathscr{C} > 0$, and Eq. (3.3) has one positive root I_2, but one can find $g(I_2) < 0$, so system (2.2) has no endemic equilibrium.

If $\beta = \nu$, then $\mathscr{A} = 0, \mathscr{B} > 0, \mathscr{C} > 0$, so Eq. (3.3) has no positive root. Therefore system (2.2) has no endemic equilibrium.

If $\beta > \nu$, then $\mathscr{A} > 0$, $\mathscr{C} > 0$, Eq. (3.3) has two positive roots I_1 and I_2, if and only if $\Delta_0 > 0$, $\mathscr{B} < 0$. Eq. (3.3) has one root of multiplicity 2, I^*, if and only if $\Delta_0 = 0$, $\mathscr{B} < 0$. We can verify that $g(I_i) > 0$, $i = 1, 2$ and $g(I^*) > 0$, so system (2.2) has two endemic equilibria $E_1 = (S(I_1), I_1, R(I_1))$ and $E_2 = (S(I_2), I_2, R(I_2))$ if and only if $\Delta_0 > 0$, $\mathscr{B} < 0$, and has one endemic equilibrium of multiplicity 2, $E^* = (S(I^*), I^*, R(I^*))$, if and only if $\Delta_0 = 0$, $\mathscr{B} < 0$. Note that $\mathscr{B} < 0$ requires $\beta > d + \nu + \mu_0$. We summarize the result in the following theorem.

Theorem 3.1. *For the system (2.2),*

(1) The disease free equilibrium E_0 always exists.
(2) If $\mathbb{R}_0 > 1$, there exists a unique endemic equilibrium E_2.
(3) If $\mathbb{R}_0 = 1$, there exists a unique endemic equilibrium E_2 provided $\mathscr{B} < 0$; otherwise there is no endemic equilibrium.
(4) If $\mathbb{R}_0 < 1$, and

(a) *if* $\beta \le d+\nu+\mu_0$, *there is no endemic equilibrium;*
(b) *if* $\beta > d+\nu+\mu_0$, *system* (2.2) *has two endemic equilibria* E_1 *and* E_2 *if and only if* $\Delta_0 > 0$, $\mathscr{B} < 0$, *and these two equilibria coalesce into* E^* *if and only if* $\Delta_0 = 0$, $\mathscr{B} < 0$; *otherwise there is no endemic equilibrium.*

3.2. Types of equilibria

Theorem 3.2. *For the system* (2.2), *the disease free equilibrium* $E_0 = (\frac{A}{d}, 0, 0)$ *is*

- $\mathbb{R}_0 < 1$: *an attracting node;*
- $\mathbb{R}_0 > 1$: *a hyperbolic saddle;*
- $\mathbb{R}_0 = 1$ *and*
  - $b > \frac{A(\mu_1-\mu_0)}{\beta(\beta-\nu)}$: *a saddle-node of codimension* 1;
  - $b < \frac{A(\mu_1-\mu_0)}{\beta(\beta-\nu)}$: *a saddle-node of codimension* 1;
  - $b = \frac{A(\mu_1-\mu_0)}{\beta(\beta-\nu)}$: *an attracting semi-hyperbolic node of codimension* 2.

The unfolding of semi-hyperbolic node of codimension 2 *is given in the bifurcation diagram of Fig. 2 with parameters* μ_1 *and* b.

Proof. For system (2.2), $-d$, $-d$ and $(d+\nu+\mu_1)(\mathbb{R}_0-1)$ are the eigenvalues of Jacobian at E_0. If $\mathbb{R}_0 < 1$, E_0 is an attracting node. If $\mathbb{R}_0 > 1$, E_0 is a hyperbolic saddle.

If $\mathbb{R}_0 = 1$, the third eigenvalue is zero. To determine the type of E_0, we linearize the system (2.2) at E_0 and diagonalize the linear part, then we obtain the following system

$$\begin{cases} \dot{X} = -\dfrac{d^2}{Ab}\left(b - \dfrac{A(\mu_1-\mu_0)}{\beta(\beta-\nu)}\right)X^2 + X\mathcal{O}\big(|Y,Z|\big) + \mathcal{O}\big(|Y,Z|^2, |X,Y,Z|^3\big), \\ \dot{Y} = -dY + \mathcal{O}\big(|X,Y,Z|^2\big), \\ \dot{Z} = -dZ + \mathcal{O}\big(|X,Y,Z|^2\big). \end{cases} \tag{3.4}$$

It is unnecessary to calculate the center manifold if $b \neq \frac{A(\mu_1-\mu_0)}{\beta(\beta-\nu)}$, and E_0 is a saddle-node.

If $b = \frac{A(\mu_1-\mu_0)}{\beta(\beta-\nu)}$, then applying the center manifold theorem to system (3.4), one can obtain

$$\begin{cases} \dot{X} = -\dfrac{d^2(d+\mu_1)^2(d+\nu+\mu_1)(d+\nu+\mu_0)}{(\mu_1-\mu_0)A^2}X^3 + \mathcal{O}\big(X^4\big), \\ \dot{Y} = -dY + \mathcal{O}\big(|X,Y,Z|^2\big), \\ \dot{Z} = -dZ + \mathcal{O}\big(|X,Y,Z|^2\big), \end{cases} \tag{3.5}$$

hence E_0 is a semi-hyperbolic attracting node. □

From Theorem 3.1, one can see the necessary condition for the existence of endemic equilibrium is $\beta > d+\nu+\mu_0$. If $\beta \le d+\nu+\mu_0$, E_0 is the unique equilibrium point and we have the following theorem.

Theorem 3.3. *For the system* (2.2), *if* $\beta \le d+\nu+\mu_0$, *the disease free equilibrium* $E_0 = (\frac{A}{d}, 0, 0)$ *is globally asymptotically stable.*

Proof. Since $\min_{I\geq 0}\{d+\nu+\mu(b,I)\} = d+\nu+\mu_0 \geq \beta$, consider the Lyapunov function $V = I$ in R^{3+} with the Liapunov derivative

$$V' = \big[-\big(d+\nu+\mu(b,I)-\beta\big)S - \big(d+\nu+\mu(b,I)\big)(I+R)\big]\frac{I}{S+I+R} \leq 0.$$

The Lyapunov–Lasalle theorem implies that solutions in D approach the largest positively invariant subset of the set $V' = 0$, i.e., the plane $I = 0$. In this plane, we have $\dot{S} = A - dS$ and $\dot{R} = -dR$ which implies $S \to \frac{A}{d}$ and $R \to 0$ as $t \to +\infty$. Thus all solutions in the plane $I = 0$ go to the disease-free equilibrium E_0. Therefore E_0 is globally asymptotically stable. □

Theorem 3.4. *For the system (2.2), if there exists exactly one simple endemic equilibrium E_2, it is an anti-saddle. If there exists exactly two simple endemic equilibria, then the equilibrium with low endemicity E_1 is a hyperbolic saddle, and the equilibrium with high endemicity E_2 is an anti-saddle.*

Proof. Denote any endemic equilibrium point as $\bar{E} = (\bar{S}, \bar{I}, \bar{R})$. The Jacobian at the endemic equilibrium point $\bar{E}$ is given by

$$J(\bar{E}) = \begin{pmatrix} -d - \frac{\beta\bar{I}(\bar{I}+\bar{R})}{(\bar{S}+\bar{I}+\bar{R})^2} & -\frac{\beta\bar{I}(\bar{S}+\bar{R})}{(\bar{S}+\bar{I}+\bar{R})^2} & \frac{\beta\bar{S}\bar{I}}{(\bar{S}+\bar{I}+\bar{R})^2} \\ \frac{\beta\bar{I}(\bar{I}+\bar{R})}{(\bar{S}+\bar{I}+\bar{R})^2} & -\mu'(\bar{I})\bar{I} - \frac{\beta\bar{S}\bar{I}}{(\bar{S}+\bar{I}+\bar{R})^2} & -\frac{\beta\bar{S}\bar{I}}{(\bar{S}+\bar{I}+\bar{R})^2} \\ 0 & \mu'(\bar{I})\bar{I} + \mu(\bar{I}) & -d \end{pmatrix}.$$

For simplicity, denote $' = \frac{\partial}{\partial I}$. We write $\mu = \mu(I) = \mu(b,I)$, and $\mu' = \mu'(I) = \frac{\partial\mu(b,I)}{\partial I}$. One can verify $\lambda = -d$ is always an eigenvalue, and the other two eigenvalues of A are the roots of

$$\lambda^2 - \mathscr{T}(\bar{I})\lambda + \mathscr{D}(\bar{I}) = 0, \tag{3.6}$$

where

$$\mathscr{T}(\bar{I}) = \frac{(\mu_1-\mu_0)b\bar{I}}{(\bar{I}+b)^2} - d\frac{A+(\beta-\nu)\bar{I}}{A-\nu\bar{I}} \quad \text{and} \quad \mathscr{D}(\bar{I}) = \frac{d\bar{I}f'(\bar{I})}{(A-\nu\bar{I})(\bar{I}+b)}.$$

Since $A - \nu\bar{I} = dN > 0$ and from Eq. (3.3), one can see $f'(I_1) < 0$, $f'(I_2) > 0$, so E_1 is a hyperbolic saddle and E_2 is an anti-saddle. If $\mathscr{T}(I_2) > 0$, E_2 is a repelling node or focus; If $\mathscr{T}(I_2) < 0$, E_2 is an attracting node or focus; If $\mathscr{T}(I_2) = 0$, E_2 could be a weak focus or a center. □

4. Bifurcations

From Theorem 3.3, we know that E_0 is globally asymptotically stable if $\beta \leq d+\nu+\mu_0$, so we will study the bifurcations when $\beta > d+\nu+\mu_0$.

4.1. Backward bifurcation and saddle-node bifurcation

Denote $\mathbb{R}_0^c = \mathbb{R}_0|_{\Delta_0=0,\mathscr{B}<0}$, then a straightforward calculation yields

$$\mathbb{R}_0^c = 1 - \frac{\mathscr{B}^2}{4\mathscr{A}Ab(d+\nu+\mu_1)},$$

therefore $0 < \mathbb{R}_0^c < 1$.

Theorem 4.1. *For the system (2.2), consider $\mathbb{R}_0$ as the bifurcation parameter.*

(1) When $\mathbb{R}_0 = 1$, system (2.2) undergoes forward bifurcation if $b > \frac{A(\mu_1-\mu_0)}{\beta(\beta-\nu)}$; system (2.2) undergoes backward bifurcation if $b < \frac{A(\mu_1-\mu_0)}{\beta(\beta-\nu)}$; system (2.2) undergoes pitchfork bifurcation if $b = \frac{A(\mu_1-\mu_0)}{\beta(\beta-\nu)}$.

(2) System (2.2) undergoes saddle-node bifurcation when $\mathbb{R}_0$ passes through $\mathbb{R}_0^c$ if $\mathscr{T}(I^*) \neq 0$. When $\mathbb{R}_0 = \mathbb{R}_0^c$, E^* is a saddle-node if $\mathscr{T}(I^*) \neq 0$, and E^* is a cusp if $\mathscr{T}(I^*) = 0$.

Proof. (1) Since $\mathbb{R}_0$ is the function of the parameters β, d, ν and μ_1, without loss of generality, we can choose μ_1 as the bifurcation parameter.

Let $\mu_1 = \beta - d - \nu + \varepsilon$, and substitute μ_1 into the system (2.2) while $\varepsilon = 0$ corresponding to $\mathbb{R}_0 = 1$. We linearize the system (2.2) at E_0, diagonalize the linear part, and apply the center manifold theorem with the parameter ε. One can obtain system (2.2) reduced on the center manifold has the following form

$$\dot{X} = -\big[\varepsilon + O\big(\varepsilon^2\big)\big]X - \left[\frac{d^2}{Ab}\left(b - \frac{A(\beta-d-\nu-\mu_0)}{\beta(\beta-\nu)}\right) + O(\varepsilon)\right]X^2 + O\big(X^3\big). \tag{4.1}$$

Denote the right side of system (4.1) as $F(X,\varepsilon)$, and we can find

$$\begin{aligned}
&F(0,0) = 0,\\
&\frac{\partial F}{\partial X}(0,0) = 0, \qquad \frac{\partial F}{\partial \varepsilon}(0,0) = 0,\\
&\frac{\partial^2 F}{\partial X \partial \varepsilon}(0,0) = -1,\\
&\frac{\partial^2 F}{\partial^2 X}(0,0) = -\frac{d^2}{Ab}\left(b - \frac{A(\beta-d-\nu-\mu_0)}{\beta(\beta-\nu)}\right) = -\frac{d^2}{Ab}\left(b - \frac{A(\mu_1-\mu_0)}{\beta(\beta-\nu)}\right).
\end{aligned}$$

Therefore system (4.1) undergoes a transcritical bifurcation if $b \neq \frac{A(\mu-\mu_0)}{\beta(\beta-\nu)}$ [18].

Note that $\frac{\partial \mathbb{R}_0}{\partial \varepsilon}|_{\varepsilon=0} = -\frac{1}{\beta} < 0$. Therefore, when $\mathbb{R}_0$ passes through $\mathbb{R}_0 = 1$, system (2.2) undergoes forward and backward bifurcation if $b > \frac{A(\mu_1-\mu_0)}{\beta(\beta-\nu)}$ and $b < \frac{A(\mu_1-\mu_0)}{\beta(\beta-\nu)}$, respectively.

If $b = \frac{A(\mu-\mu_0)}{\beta(\beta-\nu)}$, system (4.1) has the following form on the center manifold

$$\dot{X} = -\big[\varepsilon + O\big(\varepsilon^2\big)\big]X + O(\varepsilon)X^2 - \left[\frac{d^2(\beta-\nu)^2\beta(d+\nu+\mu_0)}{(\beta-d-\nu-\mu_0)A^2} + O(\varepsilon)\right]X^3 + \mathcal{O}\big(X^4\big). \tag{4.2}$$

For simplicity, we still denote the right side of system (4.1) as $F(X,\varepsilon)$, and we can find

$$\begin{aligned}
&F(0,0) = 0,\\
&\frac{\partial F}{\partial X}(0,0) = 0, \qquad \frac{\partial F}{\partial \varepsilon}(0,0) = 0,\\
&\frac{\partial^2 F}{\partial^2 X}(0,0) = 0, \qquad \frac{\partial^2 F}{\partial X\partial \varepsilon}(0,0) = -1,\\
&\frac{\partial^3 F}{\partial^3 X}(0,0) = -\frac{d^2(\beta-\nu)^2\beta(d+\nu+\mu_0)}{(\beta-d-\nu-\mu_0)A^2}\\
&\qquad\qquad = -\frac{d^2(d+\mu_1)^2(d+\nu+\mu_1)(d+\nu+\mu_0)}{(\mu_1-\mu_0)A^2} < 0.
\end{aligned}$$

Therefore system (2.2) undergoes pitchfork bifurcation if $b = \frac{A(\mu_1-\mu_0)}{\beta(\beta-\nu)}$ when $\mathbb{R}_0 = 1$ [18].

If $\varepsilon = 0$, system (4.1) and system (4.2) are exactly the first equation of system (3.4) and system (3.5), respectively.

(2) If $\mathbb{R}_0 = \mathbb{R}_0^c$, two equilibria E_1 and E_2 coalesce at E^*, and 0, $\mathscr{T}(I^*)$ and $-d$ are the three eigenvalues of the system at E^*.

If $\mathscr{T}(I^*) \neq 0$, we linearize the system at E^* and diagonalize the linear part, and obtain the following system

$$\begin{cases}
\dot{X} = \dfrac{(\mu_1-\mu_0)(A-\nu I^*)b^2d^2}{(d+\mu)(I^*+b)^3 I^*|\widetilde{T}|}X^2 + X\mathcal{O}\big(|Y,Z|\big) + \mathcal{O}\big(|Y,Z|^2, |X,Y,Z|^3\big),\\
\dot{Y} = \mathscr{T}(I^*)Y + \mathcal{O}\big(|X,Y,Z|^2\big),\\
\dot{Z} = -dZ + \mathcal{O}\big(|X,Y,Z|^2\big),
\end{cases} \tag{4.3}$$

where $\widetilde{T}$ is the non-singular linear transformation to diagonalize the linear part. From Eq. (4.3), we know E^* is a saddle-node. Combined with Theorem 3.1, system (2.2) undergoes saddle-node bifurcation when $\mathbb{R}_0$ passes through the critical value $\mathbb{R}_0^c$.

If $\mathscr{T}(I^*) = 0$, E^* is a cusp and we will elaborate this case in Section 4.3. □

As the reproduction number $\mathbb{R}_0$ is the function of the parameter μ_1, and b has the significant epidemiological meaning, we therefore choose μ_1 and b as bifurcation parameters to describe the bifurcations.

It follows from Theorem 3.1 that there exists multiple endemic equilibria if and only if

$$\mathbb{R}_0 < 1, \quad \mathscr{A} > 0, \quad \mathscr{B} < 0, \quad g\left(\frac{-\mathscr{B} \pm \sqrt{\Delta_0}}{2\mathscr{A}}\right) > 0 \quad \text{and} \quad \Delta_0 > 0. \tag{4.4}$$

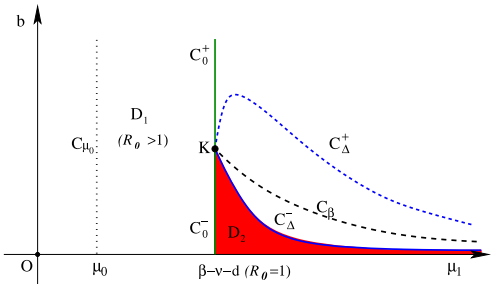

Fig. 2. The bifurcation curves in (μ_1, b) plane when $\beta > d + \nu + \mu_0$. In D_1 ($\mathbb{R}_0 > 1$), there exists a unique endemic equilibrium. There are two endemic equilibria in D_2. Two equilibria coalesce and a saddle-node bifurcation occurs on C_Δ^-. The forward bifurcation occurs on C_0^+ and backward bifurcation occurs on C_0^-. In other regions of the first quadrant there is no endemic equilibrium point.

For the condition $g(\frac{-\mathscr{B}\pm\sqrt{\Delta_0}}{2\mathscr{A}}) > 0$, it is naturally satisfied if $\mathscr{A} > 0$ holds. In fact for any root $\bar{I}$ of $f(I)$, we have $(\beta-\nu)g(\bar{I}) = (d+\mu_0)A\bar{I} + (d+\mu_1)Ab$, so $g(\bar{I}) > 0$ because $\mathscr{A} > 0$ implies $\beta - \nu > 0$.

The basic reproduction number $\mathbb{R}_0 = 1$ defines a straight line C_0 in (μ_1, b) plane,

$$C_0: \quad \mu_1 = \beta - d - \nu.$$

$\mathscr{B} = 0$ defines one branch of hyperbola $C_{\mathscr{B}}$ (see Fig. 2),

$$C_{\mathscr{B}}: \quad b = f_{\mathscr{B}}(\mu_1) \triangleq \frac{(\beta-\delta_0)A}{(\beta-\nu)(d+\nu+\mu_1)}.$$

The branch of $C_{\mathscr{B}}$ has an intersection with the C_0 at the point $K = (\beta - d - \nu, \frac{A(\mu_1-\mu_0)}{\beta(\beta-\nu)})$. It is a decreasing convex function of μ_1 with a horizontal asymptote $b = 0$.

Let

$$C_0^+ = \left\{(\mu_1, b) \,\middle|\, \mu_1 = \beta - d - \nu, b > \frac{A(\mu_1-\mu_0)}{\beta(\beta-\nu)}\right\},$$
$$C_0^- = \left\{(\mu_1, b) \,\middle|\, \mu_1 = \beta - d - \nu, 0 < b < \frac{A(\mu_1-\mu_0)}{\beta(\beta-\nu)}\right\},$$

then $C_0 = C_0^+ \cup C_0^- \cup \{K\}$. Here C_0^+ and C_0^- are two parts of C_0 separated by the point K.

Let the curve defined by $\Delta_0(\mu_1, b) = 0$ be $C_\Delta^\pm$, we solve b in term of μ_1, then

$$C_\Delta^\pm: \quad b = f_\Delta^\pm(\mu_1) \triangleq \frac{\beta(\mu_1-\mu_0) + \delta_0(\delta_1-\beta) \pm \sqrt{\beta\delta_1(\mu_1-\mu_0)(\delta_1-\beta)}}{(\beta-\nu)\delta_1^2}.$$

One can verify that $f_\Delta^\pm(\beta-d-\nu) = \frac{A(\mu_1-\mu_0)}{\beta(\beta-\nu)}$ and $f_\Delta'^\pm(\beta-d-\nu) = \pm\infty$, so the curve $C_\Delta^\pm$ is tangent to the curve C_0 at the point K. A straightforward calculation leads to

$$f_\Delta^-(\mu_1) < f_{\mathscr{B}}(\mu_1) < f_\Delta^+(\mu_1), \quad \mu_1 \in (\beta-d-\nu, \infty),$$

so the curve C_Δ^- is the one corresponding to $\Delta_0 = 0$. For the function $f_\Delta^-(\mu_1)$ one can easily find that

$$\frac{df_\Delta^-(\mu_1)}{d\mu_1} < 0, \qquad \frac{d^2 f_\Delta^-(\mu_1)}{d\mu_1^2} > 0, \qquad \mu_1 \in (\beta - d - \nu, \infty) \quad \text{and} \quad \lim_{\mu_1 \to +\infty} f_\Delta^-(\mu_1) = 0,$$

so the curve C_Δ^- under the curve $C_{\mathscr{B}}$ is convex and decreasing with the asymptote $b = 0$.

Based on the above discussion and Theorem 3.1, if we define

$$D_0 = \{(\mu_1, b) \mid b > f_\Delta^-(\mu_1), \mu_1 > \beta - d - \nu\},$$
$$D_1 = \{(\mu_1, b) \mid b > 0, \mu_0 < \mu_1 < \beta - d - \nu\},$$
$$D_2 = \{(\mu_1, b) \mid 0 < b < f_\Delta^-(\mu_1), \mu_1 > \beta - d - \nu\},$$

then there is one endemic equilibrium in region D_1 and two equilibria in region D_2. System (2.2) undergoes saddle-node bifurcation on the curve C_Δ^-. The forward bifurcation occurs on C_0^+ and backward bifurcation occurs on C_0^-. The pitchfork bifurcation occurs when transversally passing through the curve C_0 at point K. System (2.2) has a semi-hyperbolic node of codimension 2 at point K.

4.2. Hopf bifurcations

The necessary condition of Hopf bifurcation requires that $\mathscr{T}(I_2) = 0$, so firstly we study the function $\mathscr{T}(I)$. Let

$$\mathscr{T}(I) = \frac{(\mu_1 - \mu_0)bI}{(I+b)^2} - d\frac{A + (\beta - \nu)I}{A - \nu I} = -\frac{h(I)}{(A - \nu I)(I+b)^2}$$

where $h(I) = c_3 I^3 + c_2 I^2 + c_1 I + c_0$ with

$$c_3 = d(\beta - \nu), \qquad c_2 = (\mu_1 - \mu_0)b\nu + 2bd(\beta - \nu) + dA,$$
$$c_0 = b^2 dA, \qquad c_1 = b\big((\mu_0 - \mu_1 + 2d)A + (\beta - \nu)bd\big).$$

One can verify the following Lemma 4.2.

Lemma 4.2. *$\mathscr{T}(I) < 0$ for $\forall I > 0$ if $\mu_1 - \mu_0 < 4d$ or $b \geq \frac{(\mu_1 - \mu_0 - 2d)A}{(\beta - \nu)d}$.*

Lemma 4.2 asserts that small fluctuation of the recovery rate or sufficient number of hospital beds excludes the possibility of disease oscillation. In order to study the Hopf bifurcation as well as the Bogdanov–Takens bifurcation in the next section, we require that $b < \frac{(\mu_1 - \mu_0 - 2d)A}{(\beta - \nu)d}$ (i.e., $c_1 < 0$) and $\mu_1 - \mu_0 \geq 4d$.

Denote the discrimination of $h(I)$ as Δ_1. Since $c_3 > 0$, $c_2 > 0$, $c_1 < 0$ and $c_0 > 0$, $h(I)$ always has a negative real root. It is easy to verify the cubic function $h(I)$ has two humps which locate on the different sides of vertical axis, and the local maximum is obtained on the left hump, while the local minimum is obtained on the right hump. There will be zero, one or two positive roots of $h(I)$ determined by the sign of Δ_1. We denote the potential two roots as H_m and H_M with

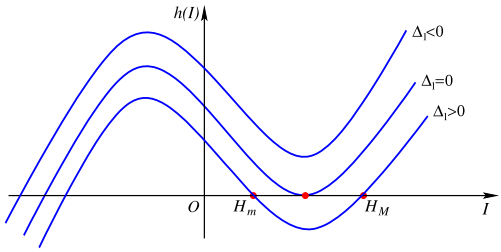

Fig. 3. Graph of $h(I)$ with different sign of Δ_1 when $c_1 < 0$. The Hopf bifurcation occurs if $I_2 = H_m$, $I_2 = H_M$ or $I_2 = H_m = H_M$. Supercritical Bogdanov–Takens bifurcation of codimension 2 occurs when $I^* = H_m$, subcritical Bogdanov–Takens bifurcation of codimension 2 occurs when $I^* = H_M$ and Bogdanov–Takens bifurcation of codimension 3 occurs when $I^* = H_m = H_M$.

$H_m \le H_M$ as shown in Fig. 3. To prove the Hopf bifurcation occurs, we need the following lemma.

Lemma 4.3.

$$\frac{\partial I_2}{\partial \mu_1} < 0, \quad \forall \mu_1 > 0 \quad \textit{and} \quad \frac{\partial I_2}{\partial b} < 0, \quad \forall b > 0.$$

Proof. From Eq. (3.3) and the expression of I_2, direct calculation leads to

$$\frac{\partial I_2}{\partial \mu_1} = -\frac{\partial f}{\partial \mu_1} \Big/ \frac{\partial f}{\partial I_2} = -\frac{(\beta - \nu) b I_2 + A b}{\sqrt{\Delta_0}} < 0,$$
$$\frac{\partial I_2}{\partial b} = \frac{1}{2\mathscr{A}} - \frac{\partial \mathscr{B}}{\partial b} + \frac{1}{\sqrt{\Delta_0}} \left(\mathscr{B} \frac{\partial \mathscr{B}}{\partial b} - 2\mathscr{A} \frac{\partial \mathscr{C}}{\partial b} \right),$$

and one can find $\frac{\partial \mathscr{B}}{\partial b} = (\beta - \nu)(d + \nu + \mu_1) > 0$. We prove $\frac{\partial I_2}{\partial b} < 0$ in two cases.

If $\mathbb{R}_0 \le 1$, then $\mathscr{C} \ge 0$ and $\frac{\partial \mathscr{C}}{\partial b} = (d + \nu + \mu_1 - \beta) A \ge 0$. Recall that Theorem 3.1 requires $\mathscr{B} < 0$, so $\frac{\partial I_2}{\partial b} < 0$. If $\mathbb{R}_0 > 1$, then $\lim_{b \to +\infty} \frac{\partial I_2(b)}{\partial b} = 0$ and

$$\frac{\partial^2 I_2}{\partial b^2} = \frac{\Delta_0^{-\frac{3}{2}}}{8\mathscr{A}} \left[2\Delta_0 \frac{\partial^2 \Delta_0}{\partial b^2} - \left(\frac{\partial \Delta_0}{\partial b} \right)^2 \right]$$
$$= \Delta_0^{-\frac{3}{2}} A^2 \beta (\beta - \nu)(\mu_1 - \mu_0)(\beta - d - \nu - \mu_1) > 0,$$

so $\frac{\partial I_2(b)}{\partial b}$ is an increasing function with supremum 0 in $(0, +\infty)$, so $\frac{\partial I_2(b)}{\partial b} < 0$ for $\forall b > 0$. □

Theorem 4.4. *A generic Hopf bifurcation could occur if $I_2 = H_m$, $I_2 = H_M$ or $I_2 = H_m = H_M$.*

Proof. We only need to verify the transversality condition. Let $\gamma = \mathscr{T}(I_2)/2$ be the real part of the eigenvalue of Eq. (3.6).

If $I_2 = H_M$ or $I_2 = H_m = H_M$, we consider μ_1 as the bifurcation parameter and fix all the other parameters. Suppose there exists $\hat{\mu}_1$ such that $\mathscr{T}(I_2(\hat{\mu}_1), \hat{\mu}_1) = 0$, and denote $' = \frac{\partial}{\partial I}$ then

$$\left.\frac{d\gamma}{d\mu_1}\right|_{\mu_1=\hat{\mu}_1} = \frac{1}{2}\left[\frac{\partial \mathscr{T}(I_2(\mu_1),\mu_1)}{\partial I_2}\frac{\partial I_2(\mu_1)}{\partial \mu_1} + \frac{\partial \mathscr{T}(I_2(\mu_1),\mu_1)}{\partial \mu_1}\right]\Bigg|_{\mu_1=\hat{\mu}_1},$$

$$\left.\frac{\partial \mathscr{T}(I_2(\mu_1),\mu_1)}{\partial I_2}\right|_{\mu_1=\hat{\mu}_1} = \frac{-h'(H_M)}{(A-\nu H_M)(H_M+b)^2} \le 0,$$

$$\left.\frac{\partial \mathscr{T}(I_2(\mu_1),\mu_1)}{\partial \mu_1}\right|_{\mu_1=\hat{\mu}_1} = \frac{bH_M}{(H_M+b)^2} > 0.$$

From Lemma 4.3 we have $\frac{\partial I_2(\mu_1)}{\partial \mu_1}|_{\mu_1=\hat{\mu}_1} < 0$, so $\frac{d\gamma}{d\mu_1}|_{\mu_1=\hat{\mu}_1} > 0$.

If $I_2 = H_m$ we consider b as the bifurcation parameter and fix all the other parameters. Suppose there exists $\hat{b}$ such that $\mathscr{T}(I_2(\hat{b}),\hat{b}) = 0$, then with the analogous argument we obtain $\frac{d\gamma}{db}|_{b=\hat{b}} < 0$ using Lemma 4.3 and the fact $H_m < \hat{b}$ which is easily proved. □

The reason we choose different parameters to unfold the Hopf bifurcation in Theorem 4.4 is that the transversality condition may fail at some points if we merely use one parameter. To prove the Hopf bifurcation can really happen, we need to prove E_2 is a weak focus. Since the system (2.2) is analytical, E_2 can only be a weak focus or center. It is important to distinguish these two types of singularities. If it is a center, then we should prove any nth order Lyapunov coefficient σ_n of E_2 vanishes, otherwise E_2 is a weak focus of order n, which means there exists an $n \in N$ such that $\sigma_i = 0$, $i = 1 \cdots n-1$ and $\sigma_n \neq 0$.

The first Lyapunov coefficient σ_1 can be calculated directly by the formula in [8] after reducing the system (2.2) on the center manifold, and we choose not to present σ_1 here due to the complexity, and we cannot give the concise explicit condition to determine the sign of σ_1. Therefore we show that σ_1 can have alternate sign or vanish by simulation as follows.

To obtain the Hopf curve in the parameter space (μ_1, b), we take the resultant of $f(I)$ and $h(I)$ with respect to I denoted as $P(\mu_1, b)$, and plot the algebraic curve $P(\mu_1, b) = 0$ by fixing parameters d, ν, A, μ_0 and β. We discard the branches of $P(\mu_1, b) = 0$ in which system (2.2) has no endemic equilibrium in the first octant, or the equilibrium with $\mathscr{T}(I) = 0$ and $\mathscr{D}(I) < 0$ corresponding to the neutral saddle curve. The neutral saddle curve is important when we consider the homoclinic bifurcation of codimension 2.

Choose $A = 20$, $\mu_0 = 10$, $d = 0.1$, $\nu = 1$, $\beta = 11.5$ and plot $P(\mu_1, b) = 0$ in (μ_1, b) plane as shown in Fig. 4(a). The algebraic curve $P(\mu_1, b) = 0$ consists of three curves and two points, green curve, blue curve, red curve, BT point and DH point. The green curve is the neutral saddle curve. Supercritical Hopf bifurcation occurs on the blue curve corresponding to $\sigma_1 < 0$, and subcritical Hopf bifurcation occurs on the red curve corresponding to $\sigma_1 > 0$.

In Fig. 4(a) we choose one point $(\mu_1, b) = (10.45, 0.022)$ marked as black asterisk below the red curve, and plot the phase portrait at this point in Fig. 4(b). One can see that as $t \to +\infty$, the trajectory (red curve) starting at $(195.3, 0.052, 4.4)$ spirals inward to the stable focus E_2 (black point), and the trajectory (blue curve) starting at $(195.7, 0.03, 3.92)$ spirals outward to the stable limit cycle (black curve). Since the Hopf bifurcation occurs on the 2-dimensional center manifold, so there is an unstable limit cycle on the center manifold. The trajectory starting at $(193, 0.08, 6.21)$ spirals inward (green curve) to the stable limit cycle (black curve).

At DH point $(\mu_1, b) = (10.427, 0.025)$, we have $\sigma_1 = 0$, so the codimension of Hopf bifurcation is at least 2, and degenerate Hopf bifurcation could happen, then we need to calculate σ_2 to determine the exact codimension of degenerate Hopf bifurcation, but the calculation of σ_2 is much more complex, and we leave this center-focus problem as future work.

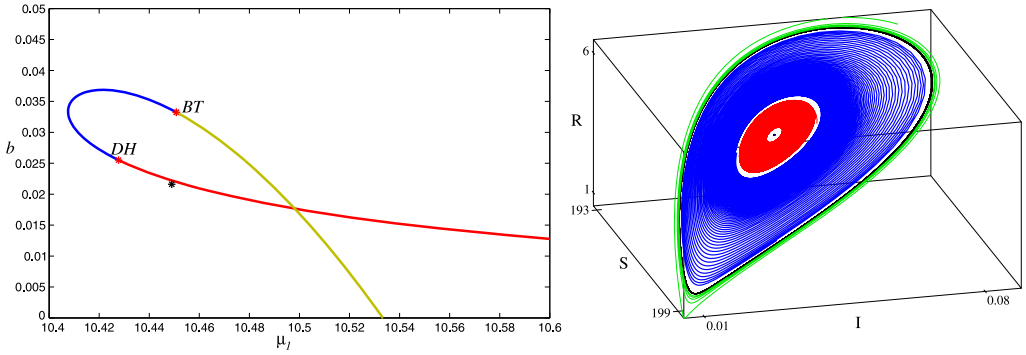

Fig. 4. (a) Algebraic curve $P(\mu_1, b) = 0$. The green curve is the neutral saddle curve. The blue curve and red curve are supercritical and subcritical Hopf bifurcation curve, respectively. σ_1 vanishes at the point DH. BT is the Bogdanov–Takens point of codimension 2. The black asterisk below the red curve is the point we choose to plot the phase portrait in (b). (b) Two limit cycles bifurcate from the weak focus E_2. (For interpretation of the references to color in this figure, the reader is referred to the web version of this article.)

In Section 4.3, we prove that the cusp type of Bogdanov–Takens bifurcation of codimension 3 occurs at E^*, which verifies that the degenerate Hopf bifurcation is exactly codimension 2 in the small neighborhood of E^* [7], so we have the following theorem.

Theorem 4.5. *Suppose that $I_2 = H_m$, $I_2 = H_M$ or $I_2 = H_m = H_M$,*

(i) If $\sigma_1 \neq 0$, the equilibrium E_2 of system (2.2) is a weak focus of order 1 and at most one limit cycle arises from the Hopf bifurcation. Furthermore, E_2 and the limit cycle are stable when $\sigma_1 < 0$; E_2 and the limit cycle are unstable when $\sigma_1 > 0$.

(ii) If $\sigma_1 = 0$ and $\sigma_2 \neq 0$, the equilibrium E_2 is a weak focus of order 2 and at most two limit cycles arise from the Hopf bifurcation, and one is stable and another is unstable.

4.3. Bogdanov–Takens bifurcation of codimension 3

It follows from Theorem 3.1 that when $\mathbb{R}_0 = \mathbb{R}_0^c$, two equilibria E_1 and E_2 coalesce at the equilibrium $E^*(S^*, I^*, R^*)$ where

$$I^* = -\frac{(d+\nu+\mu_0-\beta)A + (\beta-\nu)(d+\nu+\mu_1)b}{2(d+\nu+\mu_0)(\beta-\nu)},$$
$$S^* = \frac{A-(d+\nu+\mu(b,I^*))I^*}{d}, \qquad R^* = \frac{\mu(b,I^*)I^*}{d}.$$

One can see that $\mathscr{D}(I^*) = 0$ in Eq. (3.6). If $\mathscr{T}(I^*) \neq 0$, from Theorem 4.1, it is a saddle-node; If $\mathscr{T}(I^*) = 0$, the eigenvalues of E^* are $\lambda_{1,2} = 0$ and $\lambda_3 = -d$. In the following, we prove that the Bogdanov–Takens bifurcation of codimension 2 and codimension 3 occurs under the assumption that $\mathscr{D}(I^*) = \mathscr{T}(I^*) = 0$, or equivalently $\Delta_0 = h(I^*) = 0$.

Theorem 4.6. *Suppose $\Delta_0 = 0$, $h(I^*) = 0$ and $h'(I^*) \neq 0$, then E^* is a Bogdanov–Takens point of codimension 2, and the system (2.2) localized at E^* is topologically equivalent to*

$$\begin{cases} \dot{X} = Y, \\ \dot{Y} = X^2 + Sign\big(h'(I^*)\big)XY + \mathcal{O}\big(|X, Y|^3\big). \end{cases} \tag{4.5}$$

Proof. The translation $x = S - S^*$, $y = I - I^*$, $z = R - R^*$ brings E^* to the origin, and we obtain

$$\begin{pmatrix} \dot{x} \\ \dot{y} \\ \dot{z} \end{pmatrix} = J\big(E^*\big) \begin{pmatrix} x \\ y \\ z \end{pmatrix} + \begin{pmatrix} l_{ijk}x^i y^j z^k \\ m_{ijk}x^i y^j z^k \\ n_{ijk}x^i y^j z^k \end{pmatrix} + O\big(|x, y, z|^3\big), \tag{4.6}$$

where $0 < i, j, k \leq 2$, $i + j + k = 2$ and

$$l_{200} = \frac{\beta I^*(I^* + R^*)}{(S^* + I^* + R^*)^3}, \qquad l_{110} = -\frac{\beta(I^*R^* + 2S^*I^* + (R^*)^2 + S^*R^*)}{(S^* + I^* + R^*)^3},$$
$$l_{101} = \frac{\beta I^*(I^* + R^* - S^*)}{(S^* + I^* + R^*)^3}, \qquad l_{020} = \frac{\beta S^*(S^* + R^*)}{(S^* + I^* + R^*)^3}, \qquad l_{011} = \frac{\beta S^*(S^* - I^* + R^*)}{(S^* + I^* + R^*)^3},$$
$$l_{002} = -\frac{\beta S^* I^*}{(S^* + I^* + R^*)^3}, \qquad n_{020} = -\frac{(\mu_1 - \mu_0)b^2}{(I^* + b)^3},$$
$$n_{ijk} = 0, \quad \text{if } (i, j, k) \neq (0, 2, 0) \quad \text{and} \quad m_{ijk} = -(l_{ijk} + n_{ijk}).$$

The generalized eigenvectors of $\lambda = 0$ are

$$V_1 = \left(\frac{(\mu_1 - \mu_0)bI^*}{(I^* + b)^2} - \frac{\beta S^*}{S^* + I^* + R^*}, d, \frac{\mu_0(I^*)^2 + \mu_1 b^2 + 2b\mu_0 I^*}{(I^* + b)^2}\right)', \qquad V_2 = (-1, 1, 0)',$$

which satisfy $J(E^*)V_1 = 0$ and $J(E^*)V_2 = V_1$. $V_3 = (\frac{S^*}{I^* + R^*}, 0, 1)'$ is the eigenvector of $\lambda = -d$. Let $T = (T_{ij})_{3\times 3} = (V_1, V_2, V_3)$, then under the non-singular linear transformation

$$\begin{pmatrix} x \\ y \\ z \end{pmatrix} = T \begin{pmatrix} X \\ Y \\ Z \end{pmatrix},$$

where $|T| = -\frac{d(A - \nu I^*)^2}{\beta(d + \mu)(I^*)^2} < 0$, system (4.6) becomes

$$\begin{cases} \dot{X} = Y + L_{20}X^2 + L_{11}XY + L_{02}Y^2 + Z \cdot \mathcal{O}\big(|X, Y, Z|\big) + \mathcal{O}\big(|X, Y, Z|^3\big), \\ \dot{Y} = M_{20}X^2 + M_{11}XY + M_{02}Y^2 + Z \cdot \mathcal{O}\big(|X, Y, Z|\big) + \mathcal{O}\big(|X, Y, Z|^3\big), \\ \dot{Z} = -dZ + \mathcal{O}\big(|X, Y, Z|^2\big). \end{cases} \tag{4.7}$$

Here

$$L_{20} = -\frac{n_{020}(A - \nu I^*)d^2}{(d + \mu)I^*|T|},$$
$$M_{20} = \frac{d^2[(A - \nu I^*)\mu' I^* + (d + \mu)A][U(A - \nu I^*)^3 + \beta A(\mu A + d\nu I^* + (A - \nu I^*)\mu' I^*)]}{(A - \nu I^*)^3(d + \mu)I^*|T|},$$

$$M_{11} = -\frac{((A-\nu I^*)\mu' I^* + \mu A + 2dA)\beta d}{(A-\nu I^*)^2} - \frac{2dn_{020}((A-\nu I^*)\mu' I^* + \mu A + dA)}{(d+\mu)I^*|T|},$$

where $U = \mu' + \mu'' I^*/2$ in M_{20}. The other coefficients of quadratic terms of system (4.7) are omitted here.

According to the center manifold theorem, there exists a center manifold for system (4.7) which can be locally be represented as follows

$$W^c = \left\{(X,Y,Z) \,\middle|\, Z = H(X,Y), |X| < \varepsilon_1, |Y| < \varepsilon_2, H(0,0) = 0, DH(0,0) = 0\right\}$$

for ε_1 and ε_2 sufficiently small. Therefore one can see that $Z = \mathcal{O}(|X,Y|^2)$. In this theorem, we need not to calculate the center manifold. System (4.7) restricted to the center manifold is given by

$$\begin{cases} \dot{X} = Y + L_{20}X^2 + L_{11}XY + L_{02}Y^2 + \mathcal{O}\big(|X,Y|^3\big), \\ \dot{Y} = M_{20}X^2 + M_{11}XY + M_{02}Y^2 + \mathcal{O}\big(|X,Y|^3\big). \end{cases} \tag{4.8}$$

Using the near-identity transformation

$$X = u + \frac{1}{2}(L_{11} + M_{02})u^2 + L_{02}uv + \mathcal{O}\big(|u,v|^3\big), \qquad Y = v - L_{20}u^2 + M_{02}uv + \mathcal{O}\big(|u,v|^3\big),$$

and rewrite u, v into X, Y, we obtain

$$\begin{cases} \dot{X} = Y, \\ \dot{Y} = \overline{M}_{20}X^2 + \overline{M}_{11}XY + \mathcal{O}\big(|X,Y|^3\big), \end{cases} \tag{4.9}$$

where $\overline{M}_{20} = M_{20}$ and $\overline{M}_{11} = M_{11} + 2L_{20}$.

Consider $\overline{M}_{20}$. Note that

$$\begin{aligned} \overline{M}_{20} &= M_{20} \\ &= \frac{d^2[(A-\nu I^*)\mu' I^* + (d+\mu)A]}{(A-\nu I^*)^3(d+\mu)I^*|T|} \cdot \frac{(A-\nu I^*)^3 I^* f''(I^*)}{2(b+I^*)[A+(\beta-\nu)I^*]} \\ &= \frac{d^2[(A-\nu I^*)\mu' I^* + (d+\mu)A]}{2(d+\mu)(b+I^*)[A+(\beta-\nu)I^*]|T|} f''\big(I^*\big). \end{aligned}$$

Since $|T| < 0$, $f''(I^*) > 0$ and

$$\big(A-\nu I^*\big)\mu' I^* + (d+\mu)A > \big(A-\nu I^*\big)\mu' I^* + d\nu I^* + \mu A = \frac{d(A-\nu I^*)^2}{\beta I^*} > 0,$$

therefore $\overline{M}_{20} < 0$. Now consider $\overline{M}_{11}$. Note

$$\begin{aligned}
\overline{M}_{11} &= M_{11} + 2L_{20} \\
&= -d\frac{2n_{020}(A-\nu I^*)^2 + \beta(\mu A + 2dA + (A-\nu I^*)\mu' I^*)}{(A-\nu I^*)^2} \\
&= -d\left(\frac{2(\mu_1-\mu_0)bI^*}{(b+I^*)^3} + \mu' + \frac{d\beta A}{(A-\nu I^*)^2}\right) \\
&= -d\left[\left(d\frac{A+(\beta-\nu)I}{A-\nu I}\right)' - \left(\frac{(\mu_1-\mu_0)bI}{(b+I)^2}\right)'\right]_{I=I^*} \\
&= -\frac{d}{(A-\nu I^*)(b+I^*)^2}\, h'\big(I^*\big).
\end{aligned}$$

If $h'(I^*) \neq 0$, we make a change of coordinates and time and preserve the orientation by time

$$X \to \frac{\overline{M}_{20}}{\overline{M}_{11}^2} X, \qquad Y \to \frac{\overline{M}_{20}^2}{\overline{M}_{11}^3} Y, \qquad t \to \left|\frac{\overline{M}_{11}}{\overline{M}_{20}}\right| t,$$

then system (4.9) is topologically equivalent to the normal form (4.5). □

Theorem 4.7. *Suppose $\Delta_0 = 0$, $h(I^*) = 0$ and $h'(I^*) = 0$, then E^* is a Bogdanov–Takens point of codimension 3, and the system (2.2) localized at E^* is topologically equivalent to*

$$\begin{cases} \dot{X} = Y, \\ \dot{Y} = X^2 + EX^3Y + \mathcal{O}\big(|X,Y|^4\big)Y, \end{cases} \tag{4.10}$$

where $E < 0$.

Proof. The proof is long but standard, so we give the main idea and steps here, and omit the long calculations and the expression of M_{ij} and $\overline{M}_{ij}$ below. Firstly, expand the system (4.6) up to order 4, and diagonalize the linear part with transformation T, then

• Calculate the center manifold $Z = H(X,Y)$ up to $\mathcal{O}(|X,Y|^4)$ and reduce the system on the center manifold, then we obtain

$$\begin{cases} \dot{X} = Y + \sum\limits_{2\leq i+j\leq 4} L_{ij} X^i Y^j + \mathcal{O}\big(|X,Y|^5\big), \\ \dot{Y} = \sum\limits_{2\leq i+j\leq 4} M_{ij} X^i Y^j + \mathcal{O}\big(|X,Y|^5\big). \end{cases} \tag{4.11}$$

• Make near-identity transformation to eliminate the non-resonant terms in system (4.11), then

$$\begin{cases} \dot{X} = Y, \\ \dot{Y} = \overline{M}_{20}X^2 + \sum\limits_{3\leq i\leq 4} \big(\overline{M}_{i0}X^i + \overline{M}_{i-1,1}X^{i-1}Y\big) + \mathcal{O}\big(|X,Y|^5\big). \end{cases} \tag{4.12}$$

• Make near-identity transformation to eliminate the X^2Y term and rescale the coordinates in system (4.12), then

$$\begin{cases} \dot{X} = Y, \\ \dot{Y} = X^2 + O\big(X^3\big) + EX^3Y + \mathcal{O}\big(|X, Y|^4\big)Y. \end{cases}$$

• Let $\phi(X) = X^2 + O(X^3)$ and $\Phi(X) = \int_0^X \phi(X)dX$, eliminating the term $O(X^3)$ with change of coordinates and time $X \to (3\Phi(X))^{\frac{1}{3}}$, $Y \to Y$ and $t \to (3\Phi(X))^{-\frac{2}{3}}\phi(X)t$, then

$$\begin{cases} \dot{X} = Y, \\ \dot{Y} = X^2 + EX^3Y + \mathcal{O}\big(|X, Y|^4\big)Y, \end{cases}$$

where $E = (\overline{M}_{31}\overline{M}_{20} - \overline{M}_{30}\overline{M}_{21})/(\overline{M}_{20})^4 = (p_1\overline{M}_{20} - p_2p_3)/(\overline{M}_{20})^4$. Simplify p_1, p_2 and p_3 with the conditions $\Delta_0 = h(I^*) = h'(I^*) = 0$, and straightforward calculation leads to

$$\begin{aligned}
p_1 = &-\frac{Av^2d^3(\mu+2d)|T|}{(A-vI^*)^4} - \frac{d^4(\mu_1-\mu_0)\beta|T|b^2}{(d+\mu)(A-vI^*)(b+I^*)^4} + \frac{4d^3(\mu_1-\mu_0)b^2}{I^*(b+I^*)^5} \\
&- \frac{d^3(\mu_1-\mu_0)b\beta v^2I^*|T|}{(A-vI^*)^3(b+I^*)^2} + \frac{2d^2\beta(\mu_1-\mu_0)^3b^5[2A(\mu+d)+d(A-vI^*)]}{(d+\mu)^2(A-vI^*)^2(b+I^*)^8} \\
&+ \frac{d^2\beta(\mu_1-\mu_0)^2b^3[d(A-vI^*)^3+2A^2\beta(Ad+3Au+2dvI^*)]}{(d+\mu)I^*(A-vI^*)^4(b+I^*)^5} \\
&- \frac{2d^2\beta(\mu_1-\mu_0)^2b^4[dA\mu(3A-vI^*)+d^2(A^2-(vI^*))^2+A\mu(A\mu-dvI^*)]}{(d+\mu)^2(A-vI^*)^2(b+I^*)^6|T|^{-1}} \\
&+ \frac{2d^2\beta vI^*(\mu_1-\mu_0)^4b^6}{(d+\mu)^2(b+I^*)^{10}} - \frac{2d^2\beta^2A(\mu_1-\mu_0)^3b^4|T|[2dA+3\mu A+dvI^*]}{(d+\mu)^2I^*(A-vI^*)^3(b+I^*)^7} \\
&- \frac{2d^2Av\beta^2(I^*)^2(\mu_1-\mu_0)^4b^5|T|}{(d+\mu)^2(A-vI^*)^2(b+I^*)^9}, \\
p_2 = &\frac{d^3[(A-vI^*)\mu'I^*+(\mu+d)A][(A-vI^*)^4(\mu_1-\mu_0)b^2-A\beta v(d+\mu)I^*|T|]}{(A-vI^*)^4(d+\mu)I^*(b+I^*)^4} \\
&- \frac{d^3(\mu_1-\mu_0)\beta vb^2(A-vI^*+I)|T|}{(A-vI^*)^2(b+I^*)^3}, \\
p_3 = &\frac{\beta d^2(\mu_1-\mu_0)b^2|T|^2}{(A-vI)(b+I^*)^3} + \frac{3d^3[(A-vI^*)\mu'I^*+(\mu+d)A](\mu_1-\mu_0)b^2}{(d+\mu)(b+I^*)^4I^*} \\
&- \frac{d^2\beta v[(A-vI^*)\mu'I^*+(\mu+2d)A]|T|}{(A-vI^*)^3} + \frac{3d^3(\mu_1-\mu_0)b^2(A-vI^*)}{(d+\mu)I^*(b+I^*)^4}.
\end{aligned}$$

The sign of each factor in the expressions of p_1, p_2 and p_3 is easily determined, so one can find that $p_1 > 0$, $p_2 > 0$ and $p_3 > 0$. Since $\overline{M}_{20} < 0$, so $E < 0$ and the system (2.2) localized at E^* is topologically equivalent to system (4.10). □

Fig. 3 gives the geometrical explanation of the conditions of Hopf bifurcation and cusp type of Bogdanov–Takens bifurcation of codimension 2 and 3.

It has been shown in [7] that a generic unfolding with the parameters $\varepsilon = (\varepsilon_1, \varepsilon_2, \varepsilon_3)$ of the codimension 3 cusp singularity is C^∞ equivalent to

$$\begin{cases} \dot{X} = Y, \\ \dot{Y} = \varepsilon_1 + \varepsilon_2 Y + \varepsilon_3 XY + X^2 - X^3 Y + \mathcal{O}\big(|X, Y|^4\big) Y. \end{cases} \tag{4.13}$$

From Theorem 4.7, one can choose three parameters to unfold the codimension 3 singularity. In this paper we consider (μ_1, b, β) as bifurcation parameters and suppose that there exists a triple $(\mu_1, b, \beta) = (\mu_1^*, b^*, \beta^*)$ satisfying the conditions in Theorem 4.7 while fixing the other four parameters. In order to prove (μ_1, b, β) can really unfold the cusp type of Bogdanov–Takens bifurcation of codimension 3, we should perturb the parameters (μ_1, b, β) in the small neighborhood of (μ_1^*, b^*, β^*) in system (2.2) and by means of center manifold with parameters, changes of the coordinates and time and Malgrange preparation theorem to change the perturbed system into the normal form (4.13) while $(\varepsilon_1, \varepsilon_2, \varepsilon_3)$ is the function of (μ_1, b, β). If $\frac{\partial(\varepsilon_1, \varepsilon_2, \varepsilon_3)}{\partial(\mu_1, b, \beta)}|_{(\mu_1^*, b^*, \beta^*)} \neq 0$, then system (2.2) has the same bifurcation set with respect to (μ_1, b, β) as system (4.13) has with respect to $(\varepsilon_1, \varepsilon_2, \varepsilon_3)$, up to a homeomorphism in the parameter space.

The procedure of this proof is standard, and theoretically there is no any difficulty to make the proof. To our knowledge, for the cusp type of Bogdanov–Takens bifurcation of codimension 3, the calculations of the unfolding with three parameters are only carried out in the predator–prey system with generalized Holling type IV functional response [20] and the SIRS model with saturated incidence rate [16], while both of them are two dimensional planar systems. For our three dimensional nonlinear model, even though the unfolding with three parameters can be calculated, it is technically difficult to further simplify the expression of the unfolding and verify the condition $\frac{\partial(\varepsilon_1, \varepsilon_2, \varepsilon_3)}{\partial(\mu_1, b, \beta)}|_{(\mu_1^*, b^*, \beta^*)} \neq 0$, because of the fact that (μ_1, b, β) cannot be solved explicitly from the conditions $\Delta_0 = h(I^*) = h'(I^*) = 0$ in terms of the other parameters. Therefore we choose not to present the tediously long formula of the unfolding here since from which no analytical conclusion can be reached. On the other hand, from the simulations we can observe that all the phenomena of cusp type of Bogdanov–Takens bifurcation of codimension 3 in the neighborhood of (μ_1^*, b^*, β^*), so in the next section we present the bifurcation diagram in the (μ_1, b, β) parameter space.

For system (4.13), the plane $\varepsilon_1 = 0$ excluding the origin in the parameter space is the saddle-node bifurcation surface. When $\varepsilon_1 > 0$, system (4.13) has no equilibria, so the bifurcation surfaces are in the half space $\varepsilon_1 \leq 0$. The bifurcation diagram of system (4.13) is a cone, which can be represented by its intersection with the 2-sphere $S_{\tilde{\sigma}} = \{(\varepsilon_1, \varepsilon_2, \varepsilon_3) \mid \varepsilon_1^2 + \varepsilon_2^2 + \varepsilon_3^2 = \tilde{\sigma}^2, 0 < \tilde{\sigma} \ll 1\}$ and remove one point from the half sphere $\varepsilon_1 > 0$ as shown in Fig. 5.

On $S_{\tilde{\sigma}}$ there are three bifurcation curves: a curve H of Hopf bifurcations, a curve H_{om} of homoclinic bifurcations and a curve SN_{lc} of saddle-node bifurcations of limit cycles. The curve SN_{lc} is tangent to the H curve at H_2 and the H_{om} curve at H_{om2}. The curves H and H_{om} have first order tangency with $\partial S_{\tilde{\sigma}}$ at the points BT^+ and BT^-. In the neighborhood BT^+ and BT^-, system (4.13) is an unfolding of the cusp singularity of codimension 2. System (4.13) has a unique unstable limit cycle when the parameters lie between H and H_{om} in a small neighborhood of BT^+. System (4.13) has a unique stable limit cycle when the parameters lie between H and H_{om} in a small neighborhood of BT^-. If the parameter values are in the curved triangle CH_2H_{om2}, system (4.13) has exactly two limit cycles. The inner one is unstable and the outer one is stable. These two limit cycles coalesce on SN_{lc} where there exists a unique semi-stable limit cycle.

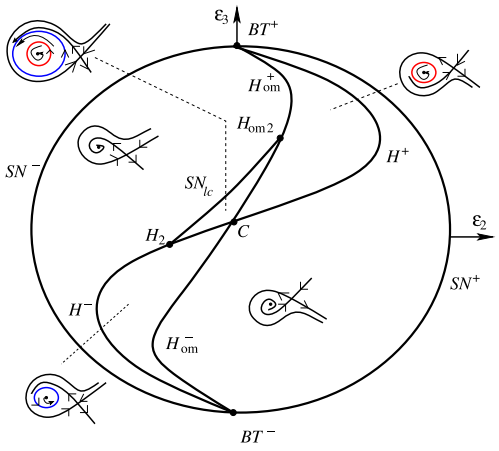

Fig. 5. Intersection of the bifurcation diagram of the cusp type of Bogdanov–Takens bifurcation of codimension 3 with S^2 minus a point.

4.4. Bifurcation diagram

In this section we consider (μ_1, b, β) as bifurcation parameters and present the bifurcation diagram based on the local study of the singular point and simulation. Suppose there exists a triple $(\mu_1, b, \beta) = (\mu_1^*, b^*, \beta^*)$ satisfying the conditions in Theorem 4.7 while fixing the other four parameters at which the cusp type of Bogdanov–Takens bifurcation of codimension 3 occurs. We give the bifurcation diagram in (μ_1, b) plane according to the sign of $h'(I^*)$ by taking slice with fixed β near the β^*. Suppose that we can find a unique $(\mu_1, b) = (\bar{\mu}_1, \bar{b})$ satisfying the conditions in Theorem 4.6, then (μ_1, b) can unfold the Bogdanov–Takens bifurcation of codimension 2.

In (μ_1, b) parameter space, the transcritical bifurcation curve C_0 and saddle-node curve SN corresponding to $\mathbb{R}_0 = 1$ and $b = f_\Delta^-(\mu_1)$ are well known in Section 4.1 and Fig. 2 as long as $\beta > d + \nu + \mu_0$. The saddle-node curve is separated by two parts if there exist a unique Bogdanov–Takens bifurcation point, the upper part connecting to the attracting semi-hyperbolic node point of codimension 2 denoted as K is the attracting saddle-node curve SN^- and the lower part stretching to infinity is the repelling saddle-node curve SN^+. Recall we preserve the orientation of the system (2.2) by time when making a sequent of changes of variables and time in Theorem 4.6, so there will be different scenarios with different sign of $h'(I^*)$. We denote the Bogdanov–Takens bifurcation point of codimension 2 with positive and negative coefficient of XY term in the normal form (4.5) as BT^+ and BT^-, respectively.

For the case $h'(I^*) < 0$, there is BT^- point on the SN curve. The Hopf bifurcation curve H and Homoclinic bifurcation curve H_{om} near the small neighborhood of BT^- are well known and they are tangent to the SN^- curve and terminate at BT^-. Based on the simulation we can plot the Hopf curve H and neutral saddle curve NS with the help of the curve $P(\mu_1, b) = 0$ introduced in Section 4.2. The homoclinic bifurcation curve H_{om} restricted in region D_2 accompanies with Hopf curve to infinity in order to compensate for change in the number of limit cycles. According to the Jordan curve theorem, the H_{om} curve will intersect the neutral saddle curve NS at least one time and the intersection is the only candidate for the degenerate Homoclinic bifurcation point H_{om2}. In the small neighborhood of BT^-, we know that the stable limit cycle bifurcating from the H curve disappears from the homoclinic loop, and from the simulation we can observe the

unstable limit cycle bifurcating from the H curve disappears from the homoclinic loop when μ_1 is large, which implies H curve and H_{om} curve switch their positions at some point C. In order to figure out the relative positions of H_{om2}, C as well as H_2, we change the value of μ_1 and plot the bifurcation diagram on $(\mathbb{R}_0, I)$ plane with different b, taking into consideration that the basic reproduction number $\mathbb{R}_0$ plays a significant role in the epidemiology and $\mathbb{R}_0$ is just a monotone decreasing function of μ_1.

From the cases (e) and (f) in Fig. 7, two limit cycles bifurcate from the semi-stable limit cycle with one disappearing from Hopf bifurcation and another disappearing from the Homoclinic loop. According to the order of these two limit cycle vanishing with different values of b, we obtain $b_{H_2} > b_C > b_{H_{om2}}$. The SN_{lc} curve and SN^+ curve should be on the different sides of H curve and H_{om} curves, so we fix the position of SN_{lc} with the endpoints H_2 and H_{om2}, then we obtain Fig. 6(a).

When $h'(I^*) \to 0^-$, the Hopf curve H moves rightward restricted in the region D_2 without changing the structure of bifurcation as shown in Fig. 6(b). Three points H_2, H_{om2} and C shrink to the BT^- point and disappear when $h'(I^*) = 0$. For the case $h'(I^*) > 0$, it is much simpler. There are one Hopf curve and one Homoclinic curve tangent to the SN^+ and stretching to infinity. Between the Hopf curve and Homoclinic curve, there is only one unstable limit cycle as shown in Fig. 6(c). These are all verified by the numerical simulations in Fig. 7.

The bifurcation diagram presented here is the simplest and compatible with all the constrains. Since the bifurcation curves for the fix points and Hopf curve are exactly determined, the only conjectural curves are the curves H_{om} and SN_{lc}. The existence and position of H_{om} is well know near the BT point. The existence of SN_{lc} is guaranteed by the codimension 3 of Bogdanov–Takens bifurcation and the position is determined by the points H_2 and H_{om2}. The phase portrait on the two dimensional center manifold in the generic parameter region and some bifurcation curves are listed in Fig. 6(d).

To confirm our conjecture, we fix four parameters $A = 20$, $\mu_0 = 10$, $d = 0.1$ and $\nu = 1$, then $(\mu_1^*, b^*, \beta^*) = (10.404, 0.0177, 11.406)$ and $E^* = (198.042, 0.018, 1.767)$ which is the cusp point of order 3.

Now we set $\beta = 11.5 > \beta^*$, then $h'(I^*) < 0$ and $BT^- = (\bar{\mu}_1, \bar{b}) = (10.450, 0.033)$. As the basic reproduction number $\mathbb{R}_0$ is significant in the epidemiology and $\mathbb{R}_0$ is a monotone decreasing function of μ_1, it is more meaningful and interesting to plot the bifurcation diagram on $(\mathbb{R}_0, I)$ plane while changing μ_1 with different b shown in Fig. 7 cases (a)–(g). Note that case (h) in Fig. 7 is a supplement which is peculiar in the bifurcation diagram Fig. 6(a) with $\beta = 12 > \beta^*$ and $BT^- = (\bar{\mu}_1, \bar{b}) = (10.914, 0.107)$.

If we change $\beta = 11.38 < \beta^*$, then $h'(I^*) > 0$ and $BT^+ = (\bar{\mu}_1, \bar{b}) = (10.411, 0.013)$. The possible cases are similar as cases (a), (b) and (g) in Fig. 7.

The cases listed in Fig. 7 are not complete and we just list some typical cases by simulation. For example, between the cases (e) and (f), there should be a case that the two limit cycles appear from saddle-node bifurcation of limit cycles, one disappearing from Hopf bifurcation and another disappearing from Homoclinic bifurcation simultaneously corresponding to the point C in Fig. 6. In fact one can list all the possible cases from bifurcation diagram in Fig. 6(a), (b) and (c).

5. Discussion and application

The parameter b (HBPR) is biologically significant as it is considered as critical index to reflect the resources of the health care system available to the public by the WHO and other health agency [2,19,21]. In this paper we consider an SIR model with standard incidence rate

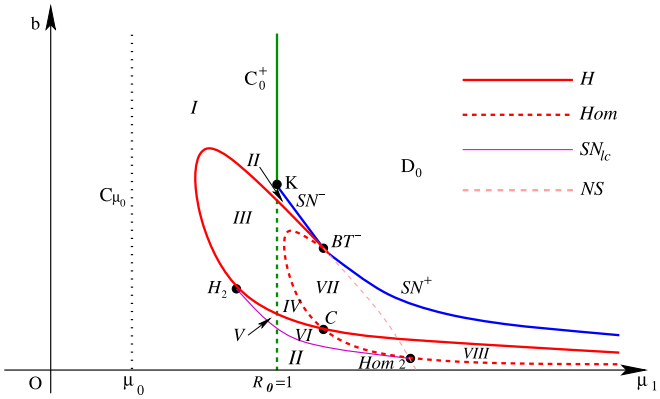

(a) Bogdanov-Takens bifurcation of codimension 2 when $h'(I^*) < 0$.

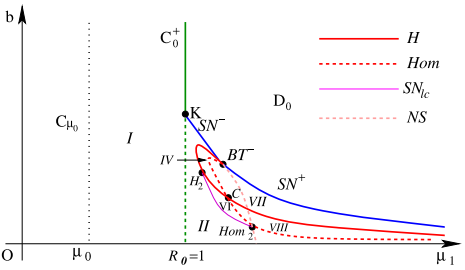

(b) Bogdanov-Takens bifurcation of codimension 2 when $-\epsilon < h'(I^*) < 0$ with $0 < \epsilon \ll 1$.

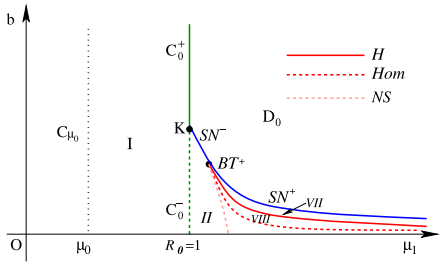

(c) Bogdanov-Takens bifurcation of codimension 2 when $h'(I^*) > 0$.

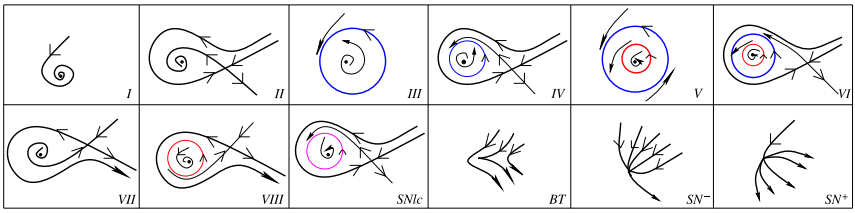

(d) Phase portraits on the two dimensional center manifold

Fig. 6. Bifurcation diagrams near the Bogdanov–Takens bifurcation of codimension 3 and the phase portraits in the generic regions of parameters and some bifurcation curves. *NS* denoted as neutral saddle curve is an auxiliary line not the bifurcation curve.

and nonlinear recovery rate incorporating the impact of the number of hospital beds. The impact of the number of hospital beds is studied in Section 4 and illustrated in the bifurcation diagram in Figs. 6 and 7.

If $\mathbb{R}_0 > 1$, E_2 is the unique equilibrium. By Lemma 4.2, it is easy to see that there is no periodic solution when b is sufficiently large such that $b > \frac{(\mu_1-\mu_0-2d)A}{(\beta-\nu)d}$, and E_2 is stable. Recall Lemma 4.3 and straightforward calculation leads to

$$\left.\frac{\partial I_2(b)}{\partial b}\right|_{b>0} < 0, \qquad \lim_{b\to+\infty}\frac{\partial I_2(b)}{\partial b} = 0 \quad \text{and} \quad \lim_{b\to+\infty} I_2(b) = \frac{\beta-(d+\nu+\mu_1)}{(\beta-\nu)(d+\nu+\mu_1)}A > 0,$$

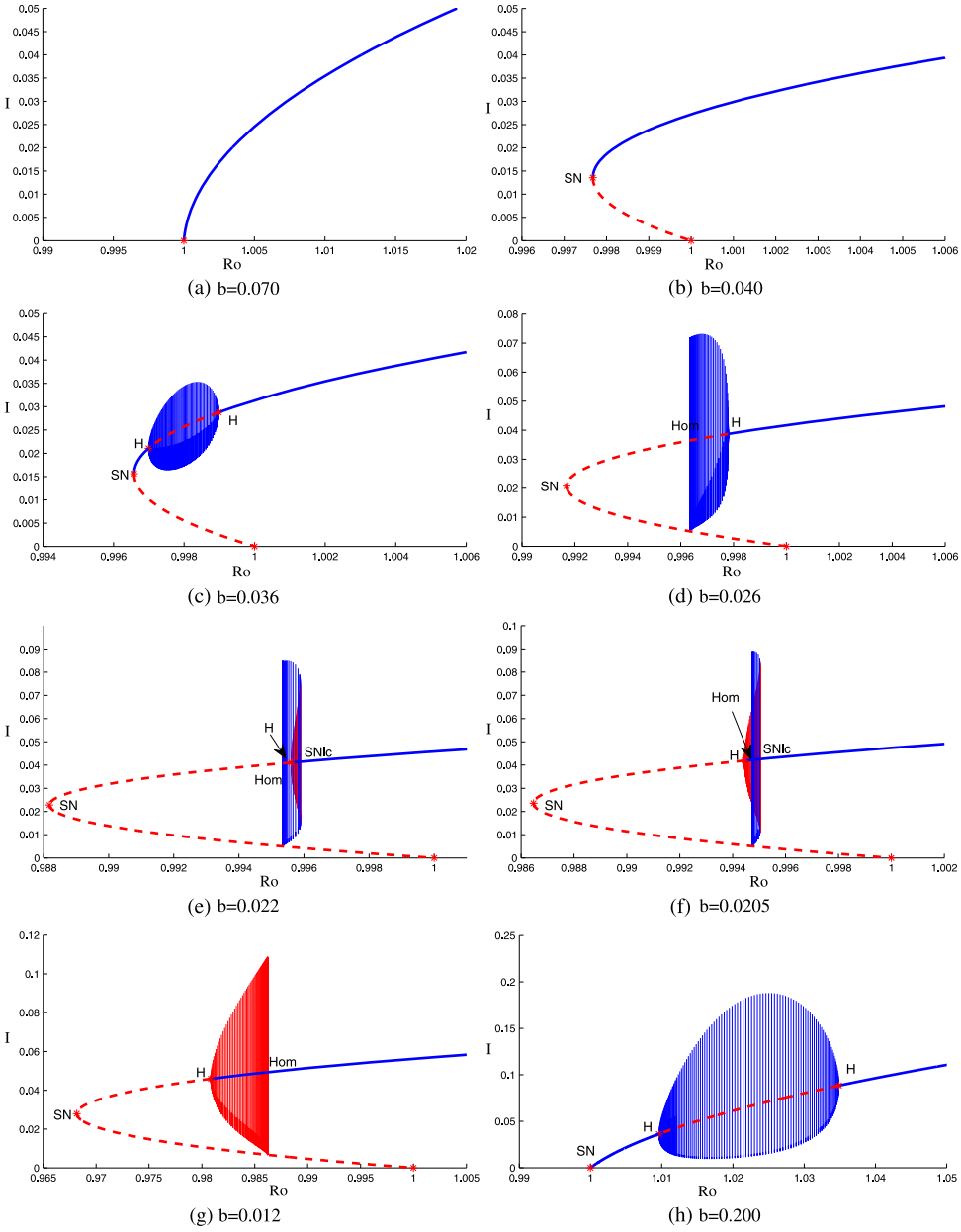

(a) b=0.070 (b) b=0.040

(c) b=0.036 (d) b=0.026

(e) b=0.022 (f) b=0.0205

(g) b=0.012 (h) b=0.200

Fig. 7. Bifurcation diagram in $(\mathbb{R}_0, I)$ plane with different b. The blue curves represent the stable fix points or limit cycles, red solid (dash) curves represent the unstable limit cycles (fix points). Forward bifurcation occurs in cases (a) and (h). Backward bifurcation and saddle-node bifurcation occur in cases (b)–(g). One stable limit cycle bifurcated from supercritical Hopf bifurcation disappears from Homoclinic bifurcation in case (d) and one unstable limit cycle bifurcated from subcritical Hopf bifurcation disappears from Homoclinic bifurcation in case (g). Two limit cycles appear from saddle-node bifurcation of limit cycles, the unstable one disappearing from subcritical Hopf bifurcation and the stable one disappearing from Homoclinic bifurcation in case (e) and (f). A stable limit cycle bifurcated from forward supercritical Hopf bifurcation disappears from the backward supercritical Hopf bifurcation in cases (c) and (h). (For interpretation of the references to color in this figure legend, the reader is referred to the web version of this article.)

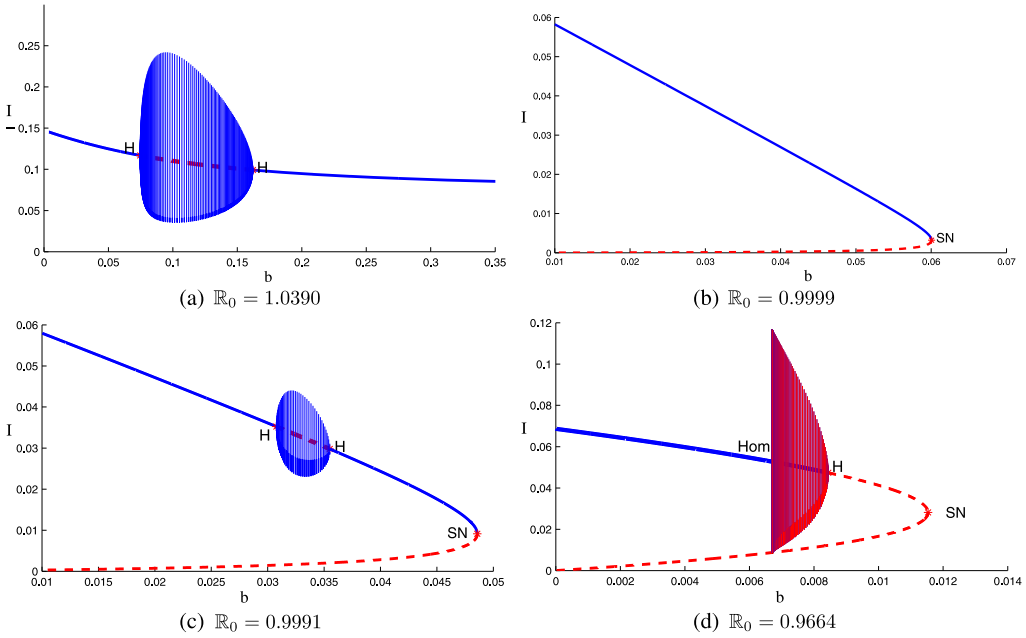

(a) $\mathbb{R}_0 = 1.0390$ (b) $\mathbb{R}_0 = 0.9999$

(c) $\mathbb{R}_0 = 0.9991$ (d) $\mathbb{R}_0 = 0.9664$

Fig. 8. Bifurcation diagram in (b, I) plane with different $\mu_1(\mathbb{R}_0)$. In case (a), $\mathbb{R}_0 > 1$, increasing the beds reduces limited number of the infectious individuals but cannot eliminate the disease. In cases (b)–(d), $\mathbb{R}_0 < 1$, disease dies out when $b > b_{crit}$ and there will be different dynamics when $b < b_{crit}$ depending on the third parameters β.

which implies $I_2(b)$ is a monotone decreasing function of b with infimum $\frac{\beta-(d+\nu+\mu_1)}{(\beta-\nu)(d+\nu+\mu_1)}A$ for $b \in (0, +\infty)$, so increasing the number of the beds can only reduce limited number of the infectious, but cannot eliminate the disease as shown in Fig. 8(a).

If $\mathbb{R}_0 < 1$, from Theorem 4.1 and Fig. 6, we can eliminate the disease when

$$b > b_{crit} \triangleq f_{\Delta}^{-}(\mu_1) = \frac{\beta(\mu_1 - \mu_0) + \delta_0(\delta_1 - \beta) - \sqrt{\beta\delta_1(\mu_1 - \mu_0)(\delta_1 - \beta)}}{(\beta - \nu)\delta_1^2}.$$

The system (2.2) presents complicated dynamics when $b < b_{crit}$, and these rich dynamics finally disappear through the saddle-node bifurcation when $b = b_{crit}$ as shown in Figs. 6 and 8(b)–(d).

In order to see the impact of the number of hospital beds more vividly, one can list all the possible bifurcation diagram in (b, I) plane from Fig. 6(a), (b) and (c) by fixing all the parameters except b. The following are some typical cases with the same parameter values as those in Fig. 7 but with different $\mu_1(\mathbb{R}_0)$.

The bifurcation analysis is carried out in this paper. Although the system (2.2) cannot be reduced to the planar system because of the variation of the total population regulated by the disease, we still have shown the backward bifurcation, saddle-node bifurcation, Hopf bifurcation and cusp type of Bogdanov–Takens bifurcation of codimension 3 can occur. By the theoretical analysis and simulation, we present the bifurcation diagram near the cusp type of Bogdanov–Takens bifurcation point of codimension 3.

The corresponding SIR model with linear recovery rate is studied by Mena-Lorca and Hethcote [14]. They show that the dynamics of the model are completely determined by $\mathbb{R}_0$, and the

disease will be eliminated if $\mathbb{R}_0 < 1$, otherwise the unique endemic equilibrium exists and is always stable. Contrasting to their work and other results for classic epidemiological models, our study suggests that the nonlinear recovery rate (2.1) can also lead to the very complicated dynamics, moreover it reveals that the basic reproduction ratio $\mathbb{R}_0$ is not enough to determine the dynamical behaviors, and three independent parameters are needed to unfold all the dynamics of the model.

Although the nonlinear recovery rate (2.1) is used for the SIR model we study, it is still applicable to other epidemiological models such as SIRS, SEIR, SIS model etc. If the disease-induced rate $\nu = 0$, all the results in this paper are still valid, even though the system (2.2) can be reduced to the planar system in this case.

Preparedness of the least number of hospital beds in case of an emerging infectious disease is a serious issue. Our results can help the public health agencies or administration arrange the appropriate number of hospital beds so as to optimize the allocation of public health resources. For a specific disease, it will be interesting and important to make use of the clinical or historical data to estimate the least number of hospital beds for control of the spread of the disease. We leave this for future work.

References

[1] R.M. Anderson, R.M. May, Infectious Diseases of Humans: Dynamics and Control, Oxford University Press, Oxford, New York, 1991.
[2] R. Boaden, N. Proudlove, M. Wilson, An exploratory study of bed management, J. Manag. Med. 13 (1999) 234–250.
[3] F. Brauer, C. Castillo-Chávez, Mathematical Models in Population Biology and Epidemiology, Springer-Verlag, New York, 2001.
[4] V. Capasso, G. Serio, A generalization of the Kermack–Mckendrick deterministic epidemic model, Math. Biosci. 42 (1978) 43–61.
[5] W.R. Derrick, P. van den Driessche, A disease transmission model in a nonconstant population, J. Math. Biol. 31 (1993) 495–512.
[6] O. Diekmann, J.A.P. Heesterbeek, Mathematical Epidemiology of Infectious Diseases: Model Building, Analysis and Interpretation, John Wiley & Sons Ltd., 2000.
[7] F. Dumortier, R. Roussarie, J. Sotomayor, Generic 3-parameter families of vector fields on the plane, unfolding a singularity with nilpotent linear part. The cusp case of codimension 3, Ergodic Theory Dynam. Systems 7 (1987) 375–413.
[8] J. Guckenheimer, P. Holmes, Nonlinear Oscillations, Dynamical Systems and Bifurcations of Vector Fields, Springer-Verlag, New York, 1983.
[9] K.P. Hadeler, P. van den Driessche, Backword bifurcation in epidemic control, Math. Biosci. 146 (1997) 15–35.
[10] H.W. Hethcote, The mathematics of infectious disease, SIAM Rev. 42 (2000) 599–653.
[11] Y. Lamontagne, C. Coutu, C. Rousseau, Bifurcation analysis of a predator–prey system with generalised Holling type III functional response, J. Dynam. Differential Equations 20 (2008) 535–571.
[12] W. Liu, Simon A. Levin, Y. Iwasa, Influence of nonlinear incidence rates upon the behavior of SIRS epidemiological models, J. Math. Biol. 23 (1986) 187–204.
[13] W. Liu, H.W. Hethcote, S.A. Levin, Dynamical behavior of epidemiological models with nonlinear incidence rates, J. Math. Biol. 25 (1987) 359–380.
[14] J. Mena-Lorca, H.W. Hethcote, Dynamic models of infectious disease as regulators of population sizes, J. Math. Biol. 30 (1992) 693–716.
[15] S. Ruan, W. Wang, Dynamical behavior of an epidemic model with a nonlinear incidence rate, J. Differential Equations 188 (2003) 135–163.
[16] Y. Tang, D. Huang, S. Ruan, W. Zhang, Coexistence of limit cycles and homoclinic loops in a SIRS model with a nonlinear incidence rate, SIAM J. Appl. Math. 69 (2008) 621–639.
[17] P. van den Driessche, J. Watmough, Reproduction numbers and sub-threshold endemic equilibria for compartmental models of disease transmission, Math. Biosci. 180 (2002) 29–48.
[18] S. Wiggins, Introduction to Applied Nonlinear Dynamical Systems and Chaos, second edition, Texts in Applied Mathematics, vol. 2, Springer-Verlag, New York, 2003.

[19] World Health Organization, World Health Statistics 2005–2011.
[20] H. Zhu, S. Campbell, G. Wolkowicz, Bifurcation analysis of a predator–prey system with nonmonotonic functional response, SIAM J. Appl. Math. 63 (2002) 636–682.
[21] http://www.who.int/whosis/indicators/hospitalbeds/en/index.html.